Feasibility of Grid-connected Solar-wind Hybrid System with Electric Vehicle Charging Station

Shakti Singh, Prachi Chauhan, and Nirbhow Jap Singh

***Abstract*—Recently, renewable power generation and electric vehicles (EVs) have been attracting more and more attention in smart grid. This paper presents a grid-connected solar-wind hybrid system to supply the electrical load demand of a small shopping complex located in a university campus in India. Further, an EV charging station is incorporated in the system. Economic analysis is performed for the proposed setup to satisfy the charging demand of EVs as well as the electrical load demand of the shopping complex. The proposed system is designed by considering the cost of the purchased energy, which is sold to the utility grid, while the power exchange is ensured between the utility grid and other components of the system. The sizing of the component is performed to obtain the least levelized cost of electricity (LCOE) while minimizing the loss of power supply probability (LPSP) by using recent optimization techniques. The results demonstrate that the LCOE and LPSP for the proposed system are measured at 0.038 $/kWh and 0.19% with a renewable fraction of 0.87, respectively. It is determined that a cost-effective and reliable system can be designed by the proper management of renewable power generation and load demands. The proposed system may be helpful in reducing the reliance on the over-burdened grid, particularly in developing countries.**

***Index Terms*—Charging station, electric vehicle (EV), optimization, solar photovoltaic (SPV) panels, wind turbine.**

I. Introduction

THE availability of limited fossil fuel reserves, climatic effects, and greenhouse gas emissions has compelled the focus toward renewable power generation in the past years. According to the Ministry of New and Renewable Energy, in India, renewable energy generation accounts for approximately 20% of the total power generation. The major contributions are from solar and wind power rather than hydro, thermal, ocean, and biomass energies [1]. Solar and wind power become prominent technologies to supply electrical load in remote and off-grid locations owing to the recent advancements in power electronic storage devices and the falling prices of the components. Reference [2] stated that solar and wind energies are freely accessible in nature and are more advantageous than other sources for power generation. However, the combination of solar and wind energies increases the complications due to their unpredictable and variable nature, which presents certain technical, environmental, and socio-economic challenges [3]. A hybrid renewable energy system can be designed using mathematical models of different components and optimization techniques [4], [5].

In recent years, extensive research has been conducted to design a solar-wind hybrid system. Reference [6] developed a solar-wind hybrid system to generate electricity, and concluded that a hybrid system could reduce the fluctuations and complexity of energy. Reference [7] simulated a solar-wind hybrid system to compute the levelized cost of electricity (LCOE) in Tripura, a north-eastern state of India. LCOE was often used to compare power generation technologies. Reference [8] developed a mathematical model of a solar-wind hybrid system to compute the output power and conducted reliability analysis to determine the performance of the system for on-grid and off-grid purposes. Reference [9] determined the size of a solar-wind hybrid system using a genetic algorithm (GA) to minimize the loss of power supply probability (LPSP) and annualized cost of the system (ACS). LPSP signified the maximum allowable limit of power loss to obtain a reliable system. ACS was another useful indicator to compare the costs of different systems because it measured their relative contributions to the total net present cost (NPC) of the system.

Reference [10] determined the size of a solar-wind hybrid system considering LCOE and LPSP. On the basis of LCOE and LPSP, to determine the optimal configuration, [11] performed economic and technical analyses of a hybrid energy system based on solar power, wind power, and battery. Reference [12] conducted an economic analysis of an electric vehicle (EV) charging station powered by solar energy. Further, it concluded that solar photovoltaic (SPV) panels could satisfy the EV demand with the LCOE of the system measured at 0.097 $/kWh at an interest rate of 6%. Reference [13] optimized the annual cost of investment and maintenance of an EV charging station based on a solar-wind hybrid system using a teaching-learning-based optimization algorithm. Reference [14] conducted an economic analysis of a solar and wind based DC microgrid that supplied power in

Manuscript received: February 8, 2019; accepted: November 6, 2019. Date of CrossCheck: November 6, 2019. Date of online publication: July 22, 2020.

S. Singh (corresponding author), P. Chauhan, and N. Singh are with the Department of Electrical and Instrumentation Engineering, Thapar Institute of Engineering and Technology, Patiala, India (e-mail: shakti. singh@thapar. edu; prachichauhan0711@gmail.com; nirbhow@thapar.edu).

DOI: 10.35833/MPCE.2019.000081

remote areas and minimized the LCOE of the system. Further, the LPSP and excess electricity were calculated. Reference [15] calculated the NPC of an EV charging station based on solar-wind hybrid power in rural areas and selected the best optimal configuration. Detailed literature on solar-wind hybrid systems can be obtained in [16]-[19].

In recent years, a significant growth of EVs and plug-in hybrid EVs has been observed in the existing power system. The integration of EVs in terms of economic analysis and power management in the renewable energy based system is an interesting and challenging research area. Reference [20] presented a comprehensive review on the research and advancement of EVs and their interaction with the grid. The feasibility of SPV-wind hybrid energy system was also discussed. The charging and discharging of EVs from a grid or microgrid result in serious problems such as high power loss, voltage deviations, and power quality problems [21].

Reference [22] emphasized that the evolution of EVs was owing to the increasing pollution from gasoline-operated vehicles and the recent development in the battery, drive motor, and charging methodology of EVs. Reference [23] developed a solar-wind hybrid system for charging EVs with simulation models. Reference [24] presented a comprehensive review based on a solar charging station and discussed different modes of charging EVs. Reference [25] proposed a hybrid solar and wind power charging station, which was implemented in Tangshan, China and developed an LPSP technique to determine the capacities of the components. Reference [26] tracked the maximum power point that can provide the maximum power to the EVs and also interfaced a DC microgrid with bi-directional DC-DC converters. Reference [27] designed an EV charging station to reduce the cost, while considering the emissions and comparing an isolated EV charging station with a grid-connected charging station. However, there were no analysis on the cost of the hybrid system. Reference [28] proposed a charging station at a work place in the Netherlands based on solar and grid-connected stations. Different scenarios for charging EVs were proposed. However, an economic analysis was not included in the work. Reference [29] performed an analysis of the demand response programs and charging of EVs by integrating them in the buses of radial distribution networks. The reliability of radial distribution systems was further elaborated by using a particle swarm optimization (PSO) algorithm with the objective of minimizing the loss of load expectation.

A variety of optimization methods such as GA [9], [30], artificial bee colony (ABC) [31], PSO [32], invasive weed optimization [33], multiplayer harmony search [34], dynamic nonlinear programming [35], biogeography-based optimization algorithm [36], simulated annealing [37], improved harmony search [38] were reported in the literature to solve various problems of engineering design. Among various available optimization algorithms, the PSO algorithm had the least mathematical complexity, whereas the ABC algorithm demonstrated the advantage of having less control parameters [39].

Researchers primarily concentrate on the control and power management of the EVs in the microgrid or grid-connected systems. However, an economic analysis considering the power exchange with the grid is one of the major parameters that must be addressed. The rapid inclusion of EVs presents both challenges and opportunities to the existing power system. The major parameters in designing a renewable energy based system include a smooth power flow between the components, reliability, and ACS of the system. In this paper, a small grid-connected solar-wind hybrid system with EVs is proposed for a small shopping complex located in a university campus in the state of Punjab in India. The primary focus is to formulate a mathematical model of a solar-wind hybrid system incorporating EVs with a grid as the backup. Further, this paper aims to minimize the power exchange with the grid. The optimal configuration of the proposed system while minimizing the ACS is performed using the ABC and PSO algorithms. A detailed comparison of the results with both algorithms is performed. A parameter sensitivity analysis is performed to analyze the impact of the algorithm parameter on the solution quality of both algorithms. Finally, a sensitivity analysis is performed to analyze the impact of the maximum grid sales and the purchase capacities on LCOE.

The remaining paper is organized into five sections. Section II explains the mathematical model along with the working methodology of the proposed solar-wind hybrid system. Section III considers the objective function and constraints of the system. Section IV presents a description of the algorithms. Section V presents the outcomes and discussions. The conclusion of the work is presented in Section VI.

II. Mathematical Model

A schematic diagram of the proposed grid-connected solar-wind hybrid system is illustrated in Fig. 1, which is a hybrid AC/DC system. In Fig. 1, PCC stands for the point of common coupling. The DC bus is connected with wind turbines, SPV panels, and a charging station, while the electrical load is connected to the AC bus. A dual converter is proposed to convert AC into DC and vice versa. The power management is more crucial in a hybrid AC/DC system compared to a single AC or DC system. Therefore, a microgrid controller is also proposed to monitor a smooth power flow between various components of the system. The detailed mathematical models of each component in the system are discussed subsequently.

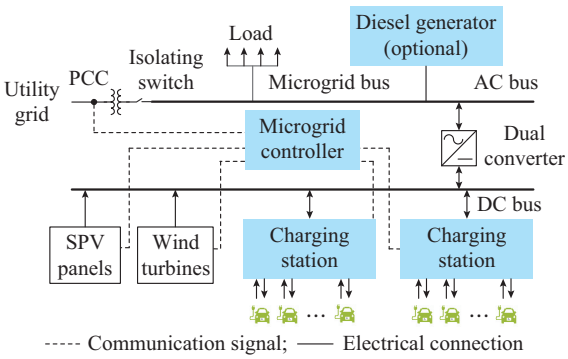

Fig. 1. Schematic diagram of proposed system.

A. Wind Turbines

The power produced by a wind turbine depends on the area through which the wind passes and the velocity of the wind. The power obtained from a wind turbine can be calculated as:

$$P_{wt}(t)=\begin{cases}0 & V(t)\le V_{cin} \text{ or } V(t)\ge V_{coff}\\ P_r^w\dfrac{V(t)-V_{cin}}{V_r-V_{cin}} & V_{cin}<V(t)<V_r\\ P_r^w & V_r\le V(t)<V_{coff}\end{cases} \tag{1}$$

where $V(t)$, V_{cin}, V_{coff}, P_r^w, V_r are the wind speeds at the required height, cut-in speed, cut-off speed, rated power of the wind turbine, and rated wind speed, respectively [40].

Wind speed at different hours of the year is represented in the form of a curve called probability density function (PDF). If a curve is plotted by considering the variable wind speeds, the area under the curve between any two wind speeds is equal to the probability of which the wind is between the two speeds. It can be expressed as:

$$\mathrm{P}(v_1\le v\le v_2)=\int_{v_1}^{v_2} f_v \mathrm{d}v \tag{2}$$

$$\mathrm{P}(0\le v\le \infty)=\int_{0}^{\infty} f_v \mathrm{d}v = 1 \tag{3}$$

where f_v is the wind speed PDF, i.e., density; and v_1 and v_2 are any two wind speeds. In wind speed statistics, the most important PDF is Weibull probability function. The Weibull probability function is defined as the starting point for characterizing the statistics of wind speed, and its expression is given as:

$$f_v=\frac{k}{c}\left(\frac{v}{c}\right)^{k-1}\exp\left(\left(-\frac{v}{c}\right)^{k}\right) \tag{4}$$

where k, c, and v are the shape parameter, scale parameter, and wind speed, respectively.

Wind speed is different over different surfaces of the earth, e.g., over a calm sea and a forest, there are different wind speeds. The variation is based on the height at which the wind speed is measured. The speed of wind at a particular height is calculated as:

$$V=V_o\left(\frac{H_{WT}}{H_o}\right)^{\alpha} \tag{5}$$

where V, V_o, and α are the wind speed at a required height H_{WT}, the wind speed at reference height H_o, and the friction coefficient, respectively. The friction coefficient depends on the terrain over which the wind blows. Generally, an approximated value of α is considered to be 1/7.

The total power generated $P_{WT}(t)$ from wind turbines is calculated as:

$$P_{WT}(t)=N_{WT}P_{wt}(t) \tag{6}$$

where N_{WT} is the number of wind turbines.

B. SPV Panel

An SPV panel is used to generate the power by harnessing solar energy. Only a small amount of solar radiation falling on the SPV panels is converted into electricity, and the rest is converted to heat. Therefore, the effect of solar radiation along with temperature on output power is considered. The output of an individual SPV panel is given as:

$$P_{sol}(t)=\frac{P_m S_m}{1000}[1-\lambda(T_{cell}-25)] \tag{7}$$

where S_m is the solar radiation.

The cell temperature and variation of power with respect to the changes in temperature is given by:

$$T_{cell}=T_{amb}+\frac{NOCT-20}{0.8}S_m \tag{8}$$

where T_{cell}, T_{amb}, and $NOCT$ are the percentage drop in power corresponding to the temperature of the cell at which power is to be calculated, ambient temperature, and cell temperature when ambient temperature is 20 °C and solar radiation is 0.8 kW/m^2, respectively.

The rated maximum power output P_m is calculated as:

$$P_m=V_m I_m \tag{9}$$

where V_m and I_m are the maximum voltage and current ratings, respectively. Further, the total power generated from SPV panels $P_{PV}(t)$ is calculated as:

$$P_{PV}(t)=N_{PV}P_{sol}(t) \tag{10}$$

where N_{PV} is the number of SPV panels.

C. EV Charging Station

The charging station is comprised of a dual converter, charging bays, and EVs. To control the power flow, the charging station is connected to a microgrid controller, which helps control the direction of the power flow at a particular time. EVs can be charged according to their state of charge (SOC), which is defined as the ratio of the available capacity to its maximum capacity when a battery is completely charged. Thus, it describes the remaining charging percentage of the battery.

Mathematically, the practical constraints imposed on the charging of EVs are described as:

$$SOC_{\min}\le SOC(t)\le SOC_{\max} \tag{11}$$

$$C_{rate}(t)\le C_{rate}^{\max} \tag{12}$$

where $SOC_{\min}$, $SOC_{\max}$, and $SOC(t)$ are the minimum, maximum, and current SOC values for a particular EV at a particular time t, respectively; and $C_{rate}(t)$ and $C_{rate}^{\max}$ are the present charging rate and maximum allowed charging rate of EVs, respectively. At any instant t, the power of the EVs at the charging station is calculated as:

$$P_{EV}(t)=\frac{E_{\max}\cdot SOC(t)}{100\Delta t} \tag{13}$$

where $E_{\max}$ is the maximum energy capacity of the vehicle; and Δt is the time interval considered as one hour. The difference in charging requirements of EVs is determined by comparing their SOC with SOC_{cr}, which is the critical SOC. In this paper, a level 2 charger with advantages of easy and user-friendly charging is considered to charge 20 EVs at a charging station.

D. Power Converter

PV panels and wind turbines feed DC power to EVs at

the charging station. However, to satisfy load demand or supply power to the grid or vice versa, converters are required. The size of the converter is chosen according to the maximum grid sales $P_{gs}^{\max}$ and purchase capacity $P_{gp}^{\max}$. The rated power of the inverter $P_{inv}(t)$ and that of the rectifier $P_{rect}(t)$ are calculated as:

$$P_{inv}(t)=P_{gs}^{\max}/\eta_{inv} \tag{14}$$

$$P_{rect}(t)=P_{gp}^{\max}\eta_{rect} \tag{15}$$

where η_{inv} and η_{rect} are the efficiency values of the inverter and rectifier, respectively.

III. Operational Strategy and Objective Function

To ensure that the solar-wind hybrid system satisfies the load power demand, as shown in Fig. 1, N_{PV} and N_{WT} must be determined. The objective function is formulated by considering the reliability and LCOE.

A. Reliability

A system is considered reliable if it has sufficient power to satisfy the load demand, which depends on LPSP. Two types of load demands are required to be satisfied: the first is the load demand of EVs $P_{DEV}(t)$ and the second is the AC load demand $P_{AC}(t)$. $P_{DEV}(t)$ at time interval t is calculated as:

$$P_{DEV}(t)=\frac{E_{\max}\cdot SOC_{cr}}{\Delta t}-P_{EV}(t) \tag{16}$$

In this paper, it is considered that the vehicles having SOC less than critical SOC are charged before 11:00 a.m.. After 11:00 a.m., the priority is given to all EVs owing to sufficient solar power availability. Further, it is assumed that all EVs arrive at 08:00 a.m. and park throughout the day. The second load demand is $P_{AC}(t)$. These demands are satisfied by two sources, i.e., SPV panels and the wind turbine. The difference between the power generated and the power demand is calculated as:

$$\Delta P(t)=P_{PV}(t)+P_{WT}(t)-P_{DEV}(t)-P_{AC}(t)/\eta_{rect} \tag{17}$$

If the sources are unable to satisfy the load demand, the power is purchased from the grid $P_{gp}(t)$ to fulfill the requirements. Moreover, if more power is available from the sources after fulfilling the demand, the power is sold to the grid $P_{gs}(t)$. However, there are limits on purchasing and selling power to the grid, which are defined as the maximum grid purchase capacity $P_{gp}^{\max}(t)$ and maximum grid selling capacity $P_{gs}^{\max}(t)$. The power cannot be purchased from the grid or sold to the grid beyond these limits. Therefore, depending on $\Delta P(t)$, the cases are formed as follows.

1) If $\Delta P(t)>0$, the total power output obtained from SPV panels and wind turbines is sufficient to charge the EVs and fulfill the requirement of the electric load. Further, the available extra power $P_{gs}(t)$ is sold to the grid, which is computed as:

$$P_{gs}(t)=(P_{PV}(t)+P_{WT}(t)-P_{DEV}(t))\eta_{inv}-P_{AC}(t) \tag{18}$$

2) If $\Delta P(t)>0$ and $\Delta P(t)>P_{gs}^{\max}(t)$, the extra power is supplied to the dump load. Dump load power $P_d(t)$ is calculated as:

$$P_d(t)=P_{PV}(t)+P_{WT}(t)-P_{DEV}(t)-(P_{AC}(t)+P_{gs}^{\max}(t))/\eta_{rect} \tag{19}$$

3) If $\Delta P(t)<0$, the power generated from SPV panels and wind turbines is not able to satisfy the power demand of EVs and the electric load. Therefore, the required power is purchased from the grid, which is given as:

$$P_{gp}(t)=(P_{DEV}(t)-P_{WT}(t)-P_{PV}(t))/\eta_{rect}+P_{AC}(t) \tag{20}$$

4) If $\Delta P(t)=0$, there is no exchange of power from the grid, and the demand of EVs and electric load is satisfied by the power generated from SPV panels and wind turbines.

When $P_{gp}(t)>P_{gp}^{\max}(t)$, both sources and grid are unable to satisfy the load demand. Consequently, power deficiency $P_{def}(t)$ occurs, which is calculated as:

$$P_{def}(t)=P_{gp}(t)-P_{gp}^{\max}(t) \tag{21}$$

$P_{def}(t)$ must be zero to ensure that the total load demand is served reliably when minimizing the LPSP. Mathematically, LPSP can be calculated as:

$$LPSP=\frac{\sum_{t=1}^{8760}P_{def}(t)}{\sum_{t=1}^{8760}(P_{AC}(t)+P_{DEV}(t))} \tag{22}$$

To solve the optimal sizing problem, the LPSP can be maintained within a specific tolerance band. In this paper, the maximum limit of LPSP is considered to be 1%. The energy management algorithm is demonstrated through a simplified flowchart to calculate the power provided to the dump load, power purchased from the grid, and power sold to the grid, as shown in Figs. 2 and 3.

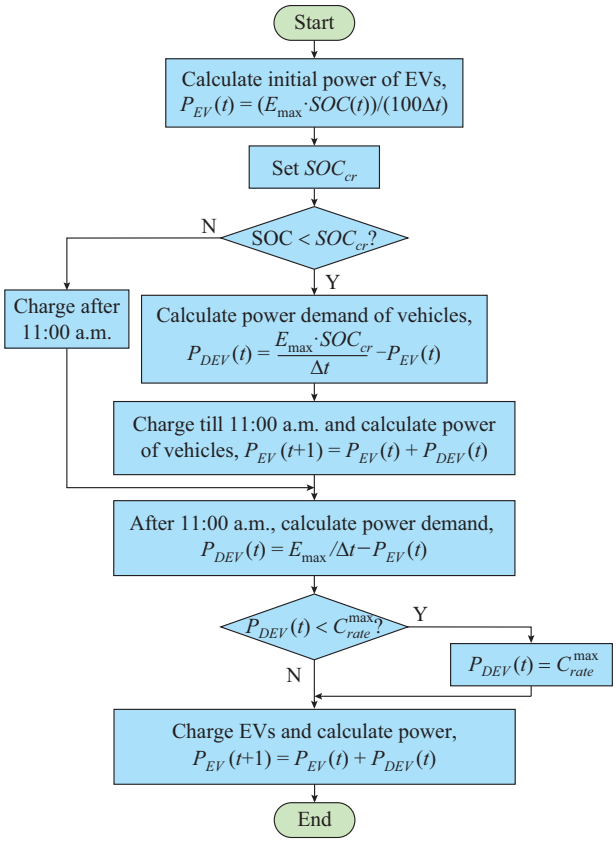

Fig. 2. Flowchart of charging methodology for EVs at charging station.

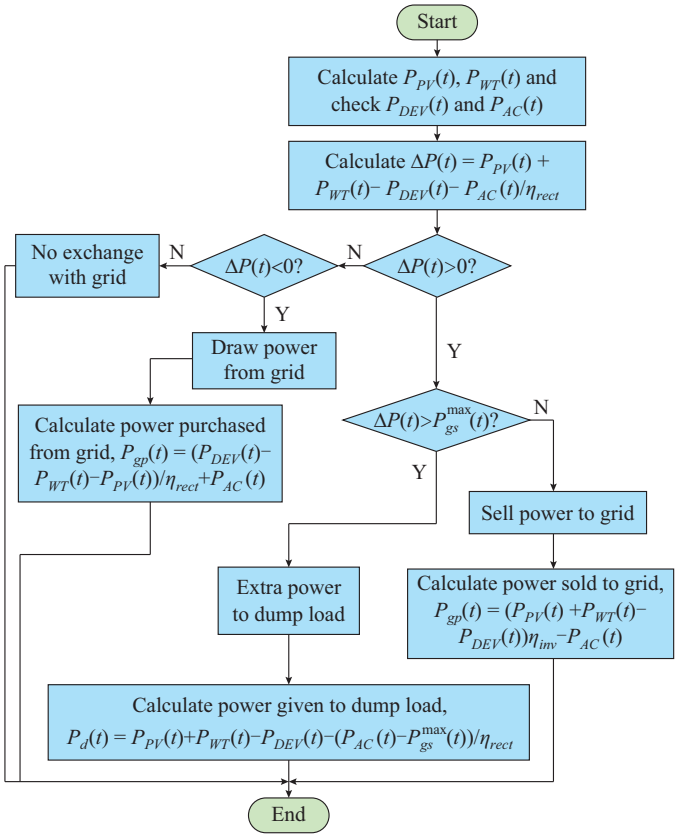

Fig. 3. Flowchart for operation strategy of proposed system.

B. LCOE

The main objective of this paper is to achieve power exchange between various components of the system and minimize LCOE of the overall proposed system. The decision variables are N_{PV} and N_{WT} required to maintain minimum LPSP and ACS. The ACS includes the costs of installing SPV panels and a wind turbine, costs of energy purchased and sold back to the grid, and costs of the converters.

$$ACS = F(N_{PV}C_{PV} + N_{WT}C_{WT} + C_{gp}E_{gp} - C_{gs}E_{gs} + C_{conv}) \quad (23)$$

where C_{PV} and C_{WT} are the costs of SPV panels and wind turbines, respectively; C_{gp} and C_{gs} are the costs of energy purchased and sold to the grid, respectively; E_{gp} and E_{gs} are the amounts of energy purchased and sold to the grid, respectively; and C_{conv} is the cost of the converters. Further, C_{PV} and C_{WT} are calculated as:

$$C_{PV} = C_{acp}^{PV} + C_{arp}^{PV} + C_{m}^{PV} + C_{sv}^{PV} \quad (24)$$

$$C_{WT} = C_{acp}^{WT} + C_{arp}^{WT} + C_{m}^{WT} + C_{sv}^{WT} \quad (25)$$

where C_{acp} is the annual capital cost; C_{arp} is the cost of replacing the components; C_m is the cost of operation and maintrnance; and C_{sv} is the salvage value; and the superscripts *PV* and *WT* denote the SPV and wind turbine, respectively.

1) Annual Capital Cost

In the annual capital cost, the installation and purchasing costs of the elements are also included. The annual capital cost of SPV panels and wind turbines are calculated by considering capital recovery factor (CRF) as:

$$C_{acp}^{PV} = C_{cp}^{PV} \cdot CRF(i,n) \quad (26)$$

$$C_{acp}^{WT} = C_{cp}^{WT} \cdot CRF(i,n) \quad (27)$$

$$CRF(i,n) = \frac{i(1+i)^n}{(1+i)^n - 1} \quad (28)$$

where C_{cp}^{PV} and C_{cp}^{WT} are the initial capital costs of SPV panels and wind turbines, respectively; and n and i are the project life time and the annual interest rate, respectively.

2) Annual Replacement Cost

Annual replacement cost includes the cost of replacing SPV panels and wind turbines if their life time is less than that of the project. The total annual cost of replacing the SPV panels and wind turbine is calculated as:

$$C_{arp}^{PV} = C_{rp}^{PV} \cdot CRF(i,n) \cdot \frac{1}{(1+i)^y} \quad (29)$$

$$C_{arp}^{WT} = C_{rp}^{WT} \cdot CRF(i,n) \cdot \frac{1}{(1+i)^y} \quad (30)$$

where C_{rp}^{PV} and C_{rp}^{WT} are the costs of replacing the SPV panel and wind turbine, respectively; and y is the life time of the panel and wind turbine in years.

3) Maintenance Cost

The maintenance cost constitutes the labor cost, cleaning cost, and cost of repairing in case of any temporary damage. The maintenance costs of SPV panels and wind turbines are calculated as:

$$C_{m}^{PV} = N_{PV}C_{m1}^{PV} \quad (31)$$

$$C_{m}^{WT} = N_{WT}C_{m1}^{WT} \quad (32)$$

where C_{m1}^{PV} and C_{m1}^{WT} are the maintenance costs of SPV panel and wind turbine, respectively.

4) Salvage Value

The cost of the remaining life for the component after the project ends is known as salvage value. The salvage values of a wind turbine and SPV panel are calculated as:

$$C_{sv}^{WT} = C_{rp}^{WT}\frac{R_{rem}}{y} \quad (33)$$

$$C_{sv}^{PV} = C_{rp}^{PV}\frac{R_{rem}}{y} \quad (34)$$

where C_{rp}^{WT} and C_{rp}^{PV} are the replacement costs of a single wind turbine and SPV panel, respectively; and R_{rem} is the remaining life.

5) Cost of Exchanging Power

The total amount of electricity purchased E_{gp} and sold back to the grid E_{gs} can be calculated as:

$$E_{gp} = \sum_{t=1}^{8760} P_{gp}(t) \quad (35)$$

$$E_{gs} = \sum_{t=1}^{8760} P_{gs}(t) \quad (36)$$

The cost of electricity purchased and sold can be calculated as:

$$C_{gp} = E_{gp}C_{g}^{P} \quad (37)$$

$$C_{gs} = E_{gs}C_{g}^{s} \quad (38)$$

where C_g^P and C_g^s are the unit costs of electricity purchased

and sold back to grid, respectively.

Moreover, the cost potency of a system can be determined by the objective function *LCOE*, which is the average cost of energy obtained from the system. It can be calculated as:

$$LCOE = \frac{ACS}{T_{total}} \tag{39}$$

where T_{total} is the total energy served.

The constraints of the objective functions are:

$$1 \le N_{PV} \le N_{PV}^{\max} \tag{40}$$

$$1 \le N_{WT} \le N_{WT}^{\max} \tag{41}$$

$$\begin{cases} P_{gp} \le P_{gp}^{\max} \\ P_{gs} \le P_{gs}^{\max} \end{cases} \tag{42}$$

$$0 \le LPSP \le 1\% \tag{43}$$

where $N_{PV}^{\max}$ and $N_{WT}^{\max}$ are the maximum numbers of SPV panels and wind turbines, respectively; and $P_{gp}^{\max}$ and $P_{gs}^{\max}$ are the maximum grid purchase and sale capacities, respectively. *LPSP* is maintained within limits while minimizing the objective function using the exterior penalty method.

IV. Solution Methodology

The proposed hybrid renewable energy system consists of more than one energy source. Therefore, this problem has multiple decision variables resulting in complex optimization problems. This problem requires the identification of energy sources for uninterrupted power supply to the EV charging station and AC load. Hence, the optimization problem incorporates economic objectives. Moreover, it requires the computation of long-term system performance to achieve the best compromise between LPSP and LCOE. LCOE is minimized using ABC and PSO algorithms as they dynamically search for an optimum system configuration while maintaining LPSP within desired limits.

A. ABC Algorithm

This algorithm explores the idea of the ABC algorithm. There are three types of bees in the ABC algorithm: employed, scout, and onlooker bees. In ABC algorithm, there are three steps in each cycle: ① employed bees search for food source or nectar amount and its location is stored in the memory; ② onlooker bees collect the information from employed bees and make the decision for selecting the best food source by doing the quality search, i.e., measuring the nectar amount of food source; ③ scout bees search for new food sources. Half of the population of bees or swarms are employed bees and the rest half are onlooker bees. For each employed bee, there is only one food source. When the food source is abandoned by the employed bees, the new food source location is randomly determined by the scout bees, and it is replaced with the abandoned food source [39], [40].

The steps for the implementation of ABC algorithm can be summed up as presented in Fig. 4, where *NS* denotes the dimension of population; *NP* denotes the colony and population sizes; and $IT^{\max}$ denotes the maximum cycle and iteration.

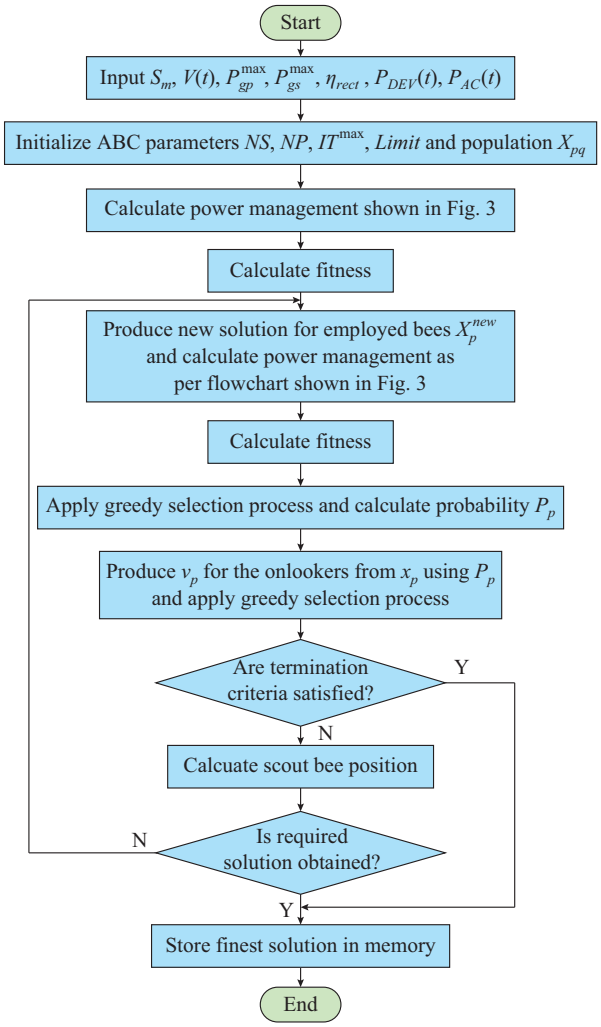

Fig. 4. Flowchart for proposed ABC algorithm.

B. PSO Algorithm

PSO contains a swarm of particles. Swarm indicates that the population and particles are candidate solutions. By optimizing the objective function, the fitness of each solution is calculated iteratively.

These candidate solutions move around the search space and their movement is directed by the swarm. And the best position in the search space becomes the upgraded position, which directs the swarm. This procedure is repeated until the best solution is obtained. At the IT^{th} iteration, the particle position p is denoted as x_p^{IT}, which moves in the search space with velocity v_p^{IT}. Therefore, the upgraded position of the particle is calculated as:

$$x_p^{IT+1} = x_p^{IT} + v_p^{IT+1} \tag{44}$$

The upgraded velocity is given by:

$$v_p^{IT+1} = W[v_p^{IT} + C_1 rand(0,1)(p_p^{IT} - x_p^{IT}) + C_2 rand(0,1)(g_p^{IT} - x_p^{IT})] \tag{45}$$

where C_1 and C_2 are the acceleration parameters; $rand(0, 1)$

is the uniformly distributed random numbers; p_p^{IT} and g_p^{IT} are the *p*-best and *g*-best, respectively; and W is an inertial weight factor, which is used for managing the capability of the search [41]. The steps for the implementation of PSO algorithm are summed up in Algorithm 1.

Algorithm 1: PSO pseudo code

Input: $S_m, V(t), P_{gs}^{\max}, P_{gp}^{\max}, \eta_{rect}$
Input: $P_{DEV}(t), P_{AC}(t)$
Input: $NS, NP, IT^{\max}$
Initialize swarm members $x_p, v_p, IT \leftarrow 0$
  while $IT < IT^{\max}$ do
    $p \leftarrow 1$
    while $p < NP$ do
      while $t \leq 8760$, $IT \leftarrow 1$ do
        Compute $P_{PV}(t)$, $P_{WT}(t)$ using (10) and (6)
        $t \leftarrow t+1$
        Power management as per flow chart shown in Fig. 3
      end while
      $f(p) \leftarrow LCOE(p) + r_k LPSP(p)$
      $p \leftarrow p+1$
    end while
    $X_p^B \leftarrow X_{\min(f(X_p^B), f(x_p))}$; $p = 1, 2, ..., NP$
    Update swarm velocity and position using (44) and (45)
    $IT \leftarrow IT+1$
  end while

The system configuration is optimized by employing both the algorithms to determine the optimal configuration that minimizes LCOE. For each system configuration observed in the search process, LPSP is determined. Therefore, for the desired LPSP, the optimal configuration can be selected by obtaining the minimum LCOE while satisfying the maximum LPSP target of 1%.

V. Results and Discussions

Figure 1 shows the sizing of different components for the system, which satisfies the charging requirements of EVs and optimizes the load demand of the shopping complex. The natural resource and electrical data of a small shopping complex located in a university campus is selected. The availability of solar radiation, wind speed, and a histogram representing wind speed frequency at the site is shown in Fig. 5. The selected data show that the site has an average wind speed of 5.9 m/s and an average solar radiation of 5.14 kWh/m^2 per day. For this particular geographical location, the data of the entire year are created by using the available resource data on the National Aeronautics and Space Administration website with hybrid optimization model for multiple energy resources software [42], [43]. The data of electricity demand of the shopping complex for one year are considered in this paper. And the shopping complex is open during the whole week. Figure 6 demonstrates the load demand of the shopping complex throughout the year, considering a 10% day-to-day load variation and 10% time-step-to-time-step variation. The hourly load demand patterns of weekends and weekdays in the summer and winter seasons are illustrated in Fig. 6(a), which demonstrate a peak load of 6.50 kW and 9 kW, respectively. During weekdays, the load demand is comparatively less than that on weekends, i.e., the peak load is 5.60 kW in winters and 8.50 kW in summers. Throughout the year, the average load demand is equal to 110 kWh per day and the overall average is measured at 4 kW. The peak demand is observed to be 12 kW and the load factor is 0.382. The load demand of an entire year is shown in Fig. 6(b) [44].

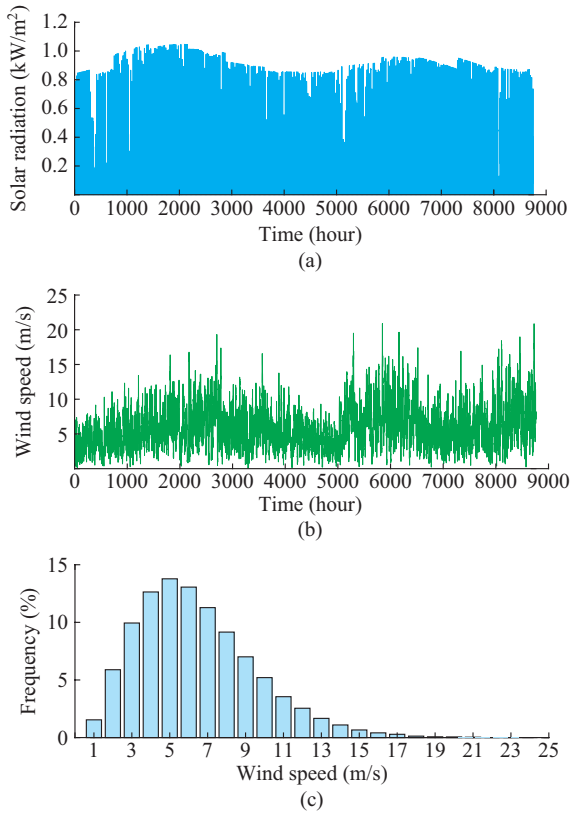

Fig. 5. Availability. (a) Solar insolation throughout the year. (b) Wind speed throughout the year. (c) Histogram representing wind speed frequency at site.

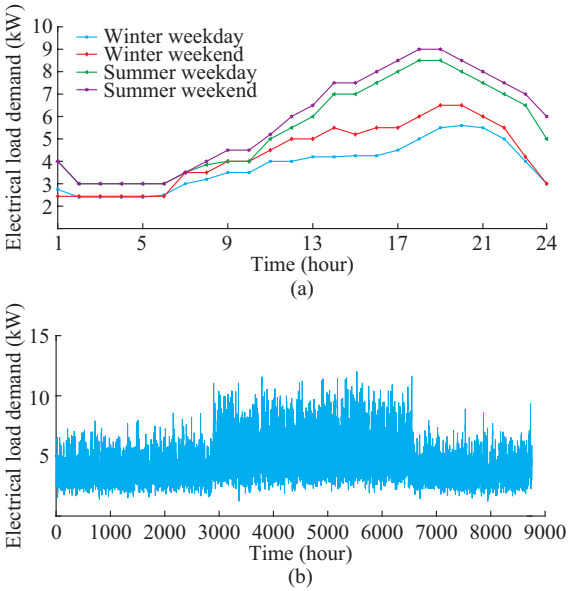

Fig. 6. Load profile. (a) During winter and summer (weekdays and weekends). (b) Throughout year after 10% variation.

Table I lists different costs and specifications associated with the components. The system is proposed for a life time of 20 years. For time value of money, an interest rate of 6% is considered. The life time of SPV panels, wind turbines, and the inverter is considered to be equal to the project life time. Therefore, no replacement is required. The simulation is conducted in MATLAB 2017a, considering the complete data of one year at 1-hour interval to calculate the power exchange and costs of the hybrid system. Moreover, the numbers of SPV panels and wind turbines are optimized by using ABC and PSO algorithms. The different parameters used in optimization technique are listed in Table II.

TABLE I
SPECIFICATION AND COST OF SYSTEM COMPONENT

Component	Parameter	Value
SPV panel	Maximum power P_{max}	100 W
	Maximum voltage V_{mp}	18 V
	Maximum power current I_{mp}	5.56 A
	Open circuit voltage V_{oc}	22.3 V
	Short-circuit current I_{sc}	6.1 A
	Number of cells	36
	Nominal operation cell temperature	45
	Capital cost and replacement cost	1084 $/kW
	O&M cost	5 $/year
	Life time	20 year
Wind turbine	Rated power	1 kW
	Capital and replacement cost	1098 $/kW
	O&M cost	2 $/kW/year
	Cut-out speed V_{co}	20 m/s
	Cut-in speed V_{cin}	5 m/s
	Hub height	50 m
	Life time	20 year
Others	DC bus voltage V_{bus}	120 V
	Project life N	20 year
	Interest rate i	6 %
Converter	Rated power	1 kW
	Rectifier and invert efficiencies	90 %
	Capital and replacement cost	127 $/kW
	O&M cost	1 $/year
	Life time	20 year
EV battery specification	Battery ampere-hour	210 Ah
	Battery type and variant	Lithiumion
	Number of modules	16
	Number of cells	48
	Battery energy capacity	5 kWh
	Maximum charging rate	0.5 kWh/h
	Maximum number of vehicles/bays	20

TABLE II
PARAMETER OF ABC ALGORITHM

Parameter	Value
Colony size	20
Dimension of colony	2
Maximum cycle	100
Employed bees (food number)	*NP*/2
Limit	100
Population size	20
Dimension of population	2
Maximum iterations	100
Inertia weight	0.4-0.9
Weighting factor	2

Table III lists the optimized results of the solar-wind hybrid system using both ABC and PSO algorithms. It is inferred from the results that by fixing the grid sales and purchase capacity to 10 kW, the ACS using ABC and PSO algorithms are 2618.3 $/year and 2953.2 $/year, respectively. Moreover, the LCOE using ABC and PSO algorithms are 0.038 and 0.043 $/kWh, respectively. It can be deduced from the table that ABC algorithm provides an acceptable solution as its LCOE is comparatively less. Figure 7 shows the convergence behaviors of both the algorithms, which can be observed in 10 initial iterations.

Table IV lists the energy production and consumption by all components of the proposed system for the configurations using ABC and PSO algorithms. In the case of energy consumption, the EV demand accounts for 25.2% of the total consumed energy, while the shopping complex accounts for 35.7% and grid sales accounts for 39%. The excess electricity is equal to 27976 kWh/year using ABC algorithm and 23488 kWh/year using PSO algorithm, respectively. The excess electricity is greater by using ABC algorithm than PSO algorithm, which is provided to the dump load. Further, LPSP from both algorithms is maintained at 0.19%.

It is inferred from the results that the ABC algorithm provides better results. Therefore, the configuration obtained from the ABC algorithm is selected. Table V lists the annualized cost analysis using the ABC algorithm. The total ACS is equal to 2618.3 $/year, which is obtained by adding the annualized capital cost of SPV panels, wind turbines, and inverters while subtracting the cost of annual grid sales. The annualized cost of components is calculated by using CRF. Further, it can be deduced from Table V that the initial costs of 36 kW SPV panels and 20 kW wind turbines is equal to $38880 and $21960, respectively. Figure 8 illustrates the complete monthly power balance throughout the year. In January, there is a deficiency in power generation with increased grid purchase.

TABLE III
OPTIMAL SIZING RESULT FOR PROPOSED SYSTEM

Algorithm	SPV capacity (kW)	Wind capacity (kW)	Converter capacity (kW)	Purchase capacity (kW)	Sales capacity (kW)	NPC ($)	ACS	LCOE
ABC	36	20	20	10	10	30021.79	2618.3	0.0380
PSO	41	16	20	10	10	33874.74	2953.2	0.0430

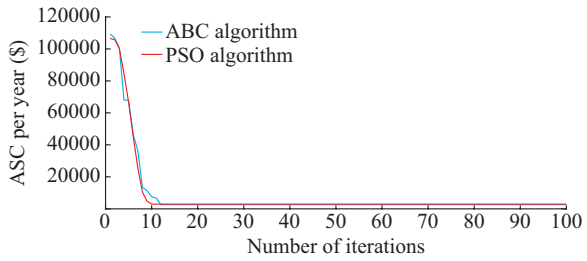

Fig. 7. Comparison of convergence characteristics of ABC and PSO algorithms.

In certain months such as April, August, and September, better solar and wind power generation is achieved, resulting in more grid sales and less grid purchases.

TABLE IV
PRODUCTION AND CONSUMPTION OF ELECTRICITY FOR A COMPLETE YEAR

Energy	Component	ABC		PSO	
		Production (kWh/year)	Consumption (%)	Production (kWh/year)	Consumption (%)
Energy production	SPV panel (DC)	60015	40.2	68350.0	48.18
	Wind turbine (DC)	80010	53.7	64008.0	45.12
	Grid purchase (AC)	8938	6.0	9491.6	6.69
	Total system	148963	100.0	141849.6	100.00
Energy consumption	EV load (DC)	28458	25.2	28458.0	25.77
	Electric load (AC)	40291	35.7	40291.0	36.49
	Grid sale	43962	39.0	41647.0	37.72
	Total system	112711	100.0	110396.0	100.00

TABLE V
COST DIVISION ACHIEVED BY ABC ALGORITHM

Component	Initial capital ($)	Capital ($/year)	Maintenance cost ($/year)	Total ($/year)
SPV panel	38880	3389.55	144.00	3533.55
Wind turbine	21960	1914.47	40.00	1954.47
Grid purchase	0	0	625.66	625.66
Grid sale	0	0	–3736.80	–3736.80
Converter	2540	221.43	20.00	241.43
Total system	63380	5525.45	–2907.14	2618.31

For better understanding of energy management in the system, two days are selected, i.e., one in winter and the other in summer. Figure 9(a) demonstrates the total power balance of one day in winter. Before 08:00 a.m., there is no charging demand for EVs and no solar and wind power generation. However, to fulfil the demand of the shopping complex, power is purchased from the grid. During the daytime hours from 11:00 a.m. to 02:00 p.m., the maximum EV demand is demonstrated and the power generation and grid sales are also at the maximum value with no power purchased from the grid. In the evening, the power purchased from the grid is at the maximum value as there is no power availability from solar and wind resources. For example, at 11:00 a.m., the electrical demand is 3.086 kW, EV demand is 18.39 kW, and wind and solar power generation values are 12.83 and 23.35 kW, respectively. The total demand is less than the generated power. Thus, the system sells 10 kW power to the grid, which is determined by the limitation in maximum sales capacity. And there is an excess power of 3.26 kW.

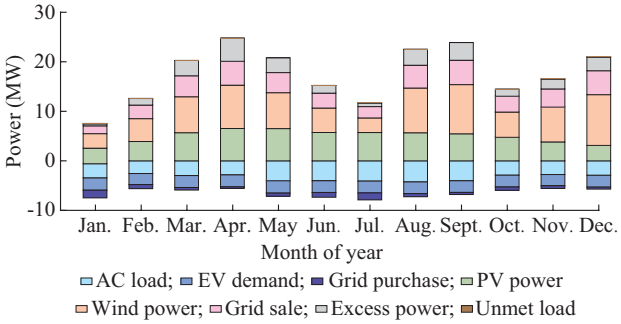

Fig. 8. Monthly power generation and consumption for whole year.

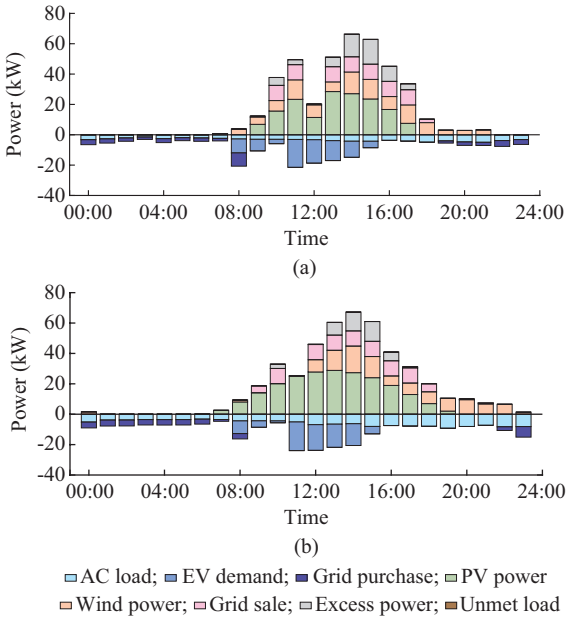

Fig. 9. One day power balance in proposed system. (a) Winter. (b) Summer.

Figure 9(b) demonstrates the total power balance of one day in summer. Because of adequate solar radiation and wind speed, there is more power generation in summer than that in winter. From 01:00 a.m. to 06:00 a.m., there is no power generation from solar and wind systems. Therefore, the demand of shopping complex is satisfied by the grid. During the daytime, the maximum solar power generation is achieved, which is sufficient to fulfil EV demand. Moreover, the excess power is sold to the grid. For example, at 01:00 a.m., the shopping complex and EV demands are 6.546 and 15.25 kW, respectively. Owing to adequate solar and wind resources, the generated power are 28.84 and 13.2 kW for solar and wind systems, respectively. The total generation is greater than the demand, therefore, the system have extra power to

sell to the grid. The total available power that can be sold to the grid is 18.40 kW. However, owing to the constraint on the maximum grid sales capacity of 10 kW, only 10 kW power is sold to the grid and the remaining 8.40 kW is supplied to the dump load. It is further evident from both the figures that there is no unsatisfied load. All the energy demands are fully satisfied by renewable power generation.

In a grid-connected system, the grid power exchange capacities, i. e., maximum sales and purchase capacities, are two major parameters. To analyze the operation of the proposed system, the effect of grid capacity verses LCOE is evaluated. Firstly, by maintaining the maximum grid purchased capacity at 10 kW, the grid sales capacity varies and LCOE is observed. Figure 10 demonstrates the variation of maximum grid sales and purchase capacities with LCOE.

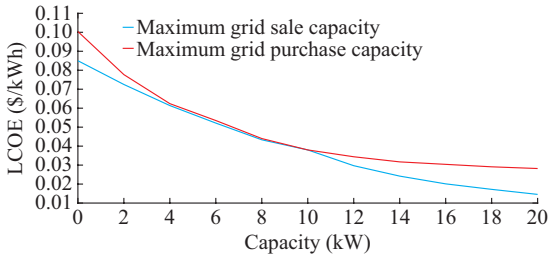

Fig. 10. Variation of levelized cost of energy with maximum grid sales and purchase capacities.

It can be observed that LCOE decreases significantly as the maximum grid sales increases. Further, by maintaining the maximum grid sales capacity, i.e., 10 kW, the maximum grid purchase capacity varies. Moreover, the results are plotted in Fig. 10. The results clearly depict that with increasing grid purchase capacity, the LCOE of the system decreases.

A. Special Case: Uncertainty in Behavior of EVs

The above case study is proposed considering a time limit in the arrival and departure of EVs at the charging station within office hours. To prove the efficiency of the proposed model, another case study is analyzed and presented in this subsection. A more generalized and flexible, 24 × 7 charging station is considered. Further, it is assumed that the arrival and departure time of the EVs is uncertain. No charging preference is given to any of the EVs, and it is assumed that the charging occur as per the user requests. The maximum grid sales and purchase capacities are maintained similar to the previous case study.

Table VI lists the results obtained using both algorithms. It is evident from the results that the LCOE demonstrate a marginal increase compared to the previous case. The system sells 11957 kWh/year power to the grid compared to 43962 kWh/year in the previous case, and purchases 19168 kWh/year from the grid compared to 8938 kWh/year in the previous case. The system in the previous case study utilizes more solar power, owing to more power generation during the daytime.

TABLE VI
OPTIMAL SIZING RESULT FOR PROPOSED HYBRID SYSTEM IN A SPECIAL CASE

Algorithm	SPV capacity (kW)	Wind capacity (kW)	Converter capacity (kW)	Purchase capacity (kW)	Sales capacity (kW)	NPC ($)	ACS	LCOE ($/kWh)
ABC	5	10	20	10	10	23893	2083.12	0.0399
PSO	6	9	20	10	10	25885	2256.83	0.0432

Figure 11(a) and (b) demonstrates the power balance for the two days, i.e., one in winter and the other in summer.

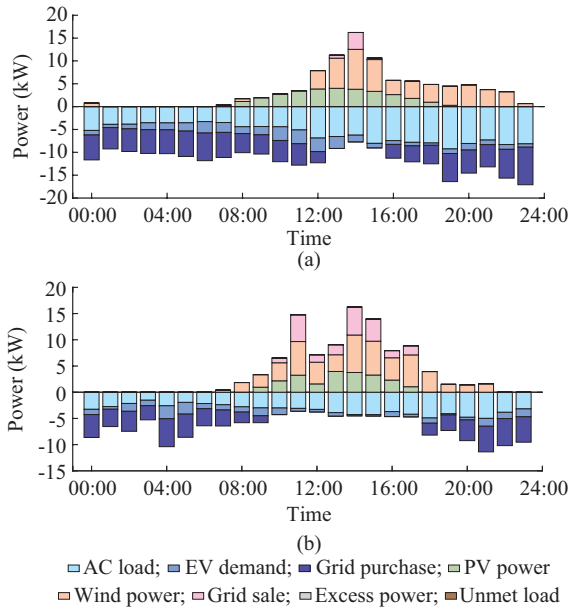

Fig. 11. One-day power balance. (a) Winter. (b) Summer.

The power balance shows that the EV load is distributed throughout the day and night compared to the previous case study. The second case is more generic and can be applied to any charging station powered by renewable sources, and the grid can be treated as a backup. LCOE is competitive in both case studies. However, the system will be more grid dependent rather than depending on renewable power sources in the second case.

B. Parameters Considered for Sensitivity Analysis

The performance of metaheuristic algorithms is dependent on the control parameter. Therefore, to verify the effectiveness of the considered algorithms, a comparison of the results of the PSO and ABC algorithms is performed with respect to variations in different control parameters. In both algorithms, the values of the common parameters used such as population size and total evaluation number are chosen to be the same, i. e., 20 and 100, respectively. The other specific parameters considered for sensitivity analysis in the case of PSO are cognitive and social components, which are represented in this paper as C_1 and C_2, respectively. In the experiments, the cognitive and social components are both set to be 2.0. In the case of the ABC algorithm, excluding the com-

mon parameters, only one control parameter is considered as *Limit*. The aforementioned parameters vary by ±10% of the standard parameter values proposed in the literature [45]. Table VII lists the experimental study undertaken for parameter sensitivity analysis of the considered problem. The obtained solution depicts small variations around the mean value. Moreover, the relative deviation from the minimum ACS is less than 1%. A similar trend is observed in both algorithms.

TABLE VII
ANALYSIS OF PARAMETER SENSITIVITY

Algorithm	Parameter	Scope	Step	ACS				
				Mean ($/year)	Minimum ($/year)	Maximum ($/year)	Standard deviation ($/year)	Variation of ACS (%)
PSO	C_1	0-4	0.2	2957.72	2953.2	2963.0	3.259	0.1101
	C_2	0-4	0.2	2957.62	2953.2	2967.8	3.325	0.1124
ABC	*Limit*	0-200	20.0	2629.39	2618.3	2639.0	5.975	0.2272

VI. CONCLUSION

Hybrid renewable energy systems have the potential to provide electricity to grid and off-grid locations economically and reliably. The efficiency of the system is enhanced if the renewable energy systems are integrated with the grid. In this paper, a detailed mathematical model and operation strategy are presented to deduce the component sizing of solar-wind hybrid system that incorporates an EV charging station. The optimal configuration consists of solar capacity of 36 kW and wind capacity of 20 kW along with grid sales and purchase capacities of 10 kW. The EV demand of 28 MWh/year and the shopping arcade demand of 40 MWh/year are completely managed by the renewable energy sources and the grid. Excess electricity of 27 MWh/year is given to the dump load. The energy sold to the grid is 43 MWh/year, which is much higher than the energy purchased from the grid, i.e., 8 MWh/year. LCOEs obtained from ABC and PSO algorithms are measured to be 0.038 and 0.043 $/kWh, respectively. LCOEs using both algorithms are highly competitive with the cost of energy purchased from the grid, while maintaining the LPSP to be 0.19%.

Moreover, a more generic case study is considered by relaxing the time constraints, and the system is satisfactorily economical. However, the grid dependency increases in this case. Further, a sensitivity impact analysis on the maximum grid sales and purchase capacities on the LCOE is performed. In a grid-connected system, the maximum grid sales and purchase capacities demonstrate a significant impact on LCOE and ACS of the system. Finally, a parameter sensitivity analysis is performed to analyze the impact of the algorithm parameters on the solution quality of both algorithms. The obtained solution shows minor variations around the mean value, and the relative deviation from the minimum ACS is less than 1%. The proposed system will be helpful in promoting renewable energy sources in smart grid and can reduce the dependence of a small community on the grid.

REFERENCES

[1] Ministry of New and Renewable Energy Annual Report. (2019, Dec.) [Online]. Available: https://mnre.gov.in/knowledge-center/publication

[2] M. Nehrir, C. Wang, K. Strunz *et al*., "A review of hybrid renewable/alternative energy systems for electric power generation: configurations, control, and applications," *IEEE Transactions on Sustainable Energy*, vol. 2, no. 4, pp. 392-403, May 2011.

[3] X. Chen, M. B. Mcelroy, Q. Wu *et al*., "Transition towards higher penetration of renewables: an overview of interlinked technical, environmental and socio-economic challenges," *Journal of Modern Power Systems and Clean Energy*, vol. 7, no. 1, pp. 1-8, Aug. 2019.

[4] W. Zhou, C. Lou, Z. Li *et al*., "Current status of research on optimum sizing of stand-alone hybrid solar-wind power generation systems," *Applied Energy*, vol. 87, no. 2, pp. 380-389, Feb. 2010.

[5] A. Kanase-Patil, R. Saini, and M. Sharma, "Integrated renewable energy systems for off grid rural electrification of remote area," *Renewable Energy*, vol. 35, no. 6, pp. 1342-1349, Jun. 2010.

[6] V. J. Babrekar, S. D. Bandawar, and A. R. Behade, "Review paper on hybrid solar-wind power generator," *International Journal of Computer Applications*, vol. 165, no. 5, pp. 36-40, May 2017.

[7] S. Bhattacharjee and S. Acharya, "PV-wind hybrid power option for a low wind topography," *Energy Conversion and Management*, vol. 89, pp. 942-954, Jan. 2015.

[8] G. Tina, S. Gagliano, and S. Raiti, "Hybrid solar/wind power system probabilistic modelling for long-term performance assessment," *Solar Energy*, vol. 80, no. 5, pp. 578-588, May 2006.

[9] H. Yang, W. Zhou, L. Lu *et al*., "Optimal sizing method for stand-alone hybrid solar-wind system with LPSP technology by using genetic algorithm," *Solar Energy*, vol. 82, no. 4, pp. 354-367, Apr. 2008.

[10] A. Kaabeche, M. Belhamel, and R. Ibtiouen, "Sizing optimization of grid-independent hybrid photovoltaic/wind power generation system," *Energy*, vol. 36, no. 2, pp. 1214-1222, Feb. 2011.

[11] S. Diaf, M. Belhamel, M. Haddadi *et al*., "Technical and economic assessment of hybrid photovoltaic/wind system with battery storage in corsica island," *Energy Policy*, vol. 36, no. 2, pp. 743-754, Feb. 2008.

[12] B. Ye, J. Jiang, L. Miao *et al*., "Feasibility study of a solar-powered electric vehicle charging station model," *Energies*, vol. 8, no. 11, pp. 13265-13283, Nov. 2015.

[13] A. Koochaki, M. Divandari, E. Amiri *et al*., "Optimal design of solar-wind hybrid system using teaching-learning based optimization applied in charging station for electric vehicles," in *Proceedings of IEEE Transportation Electrification Conference and Expo*, Long beach, USA, Jun. 2018, pp. 1-6.

[14] R. Kaur, V. Krishnasamy, and N. K. Kandasamy, "Optimal sizing of-wind-PV-based DC microgrid for telecom power supply in remote areas," *IET Renewable Power Generation*, vol. 12, no. 7, pp. 859-866, May 2018.

[15] M. Nizam and F. R. Wicaksono, "Design and optimization of solar, wind, and distributed energy resource hybrid power plant for electric vehicle charging station in rural area," in *Proceedings of 5th International Conference on Electric Vehicular Technology*, Surakarta, Indonesia, Oct. 2018, pp. 41-45.

[16] M. Habib, S. Said, M. El-Hadidy *et al*., "Optimization procedure of a hybrid photovoltaic wind energy system," *Energy*, vol. 24, no. 11, pp. 919-929, Nov. 1999.

[17] J. Li, W. Wei, and J. Xiang, "A simple sizing algorithm for stand-alone PV/wind/battery hybrid microgrids," *Energies*, vol. 5, no. 12, pp. 5307-5323, Dec. 2012.

[18] H. Yang, L. Lu, and W. Zhou, "A novel optimization sizing model for hybrid solar-wind power generation system," *Solar Energy*, vol. 81, no. 1, pp. 76-84, Jan. 2007.

[19] G. Bekele and G. Boneya, "Design of a photovoltaic-wind hybrid pow-

er generation system for ethiopian remote area," *Energy Procedia*, vol. 14, pp. 1760-1765, 2012.
[20] F. Mwasilu, J. J. Justo, E.-K. Kim *et al*., "Electric vehicles and smart grid interaction: a review on vehicle to grid and renewable energy sources integration," *Renewable and Sustainable Energy Reviews*, vol. 34, pp. 501-516, Jun. 2014.
[21] S. Singh, S. Jagota, and M. Singh, "Energy management and voltage stabilization in an islanded microgrid through an electric vehicle charging station," *Sustainable Cities and Society*, vol. 41, pp. 679-694, Jun. 2018.
[22] H. C. Yu and C. G. Lu, "Recent development of electric vehicles," *Applied Mechanics and Materials*, vol. 490, pp. 968-971, Jan. 2014.
[23] C. Chellaswamy, V. Nagaraju, and R. Muthammal, "Solar and wind energy based charging station for electric vehicles," *International Journal of Advanced Research in Electrical Electronics and Instrumentation Engineering*, vol. 7, no. 1, pp. 313-324, Jan. 2018.
[24] S. Khan, A. Ahmad, F. Ahmad *et al*., "A comprehensive review on solar powered electric vehicle charging system," *Smart Science*, vol. 6, no. 1, pp. 54-79, Dec. 2017.
[25] H. Li, H. Liu, A. Ji *et al*., "Design of a hybrid solar-wind powered charging station for electric vehicles," in *Proceedings of International Conference on Materials for Renewable Energy and Environment*, Chengdu, China, Aug. 2014, pp. 977-981.
[26] M. Nashed and I. Edwar, "Wind/PV hybrid of DC electric vehicle charging station with bi-directional converter," in *Proceedings of World Engineering Conference and Convention*, Kyoto, Japan, Dec. 2015, pp. 1-6.
[27] O. Hafez and K. Bhattacharya, "Optimal design of electric vehicle charging stations considering various energy resources," *Renewable Energy*, vol. 107, pp. 576-589, Jul. 2017.
[28] G. C. Mouli, P. Bauer, and M. Zeman, "System design for a solar powered electric vehicle charging station for workplaces," *Applied Energy*, vol. 168, pp. 434-443, Apr. 2016.
[29] O. Sadeghian, M. Nazari-Heris, M. Abapour *et al*., "Improving reliability of distribution networks using plug-in electric vehicles and demand response," *Journal of Modern Power Systems and Clean Energy*, vol. 7, no. 5, pp. 1189-1199, May 2019.
[30] A. E. S. A. Nafeh, "Optimal economical sizing of a PV-wind hybrid energy system using genetic algorithm," *International Journal of Green Energy*, vol. 8, no. 1, pp. 25-43, Feb. 2011.
[31] M. R. Javadi, A. Jalilvand, R. Noroozian *et al*., "Optimal design and economic assessment of battery based stand-alone wind/PV generating system using ABC," in *Proceedings of the 3rd Conference on Thermal Power Plants*, Tehran, Iran, Jan. 2011, pp. 1-7.
[32] L. Wang and C. Singh, "Multicriteria design of hybrid power generation systems based on a modified particle swarm optimization algorithm," *IEEE Transactions on Energy Conversion*, vol. 24, no. 1, pp. 163-172, Jan. 2009.
[33] M. Kharrich, M. Akherraz, and Y. Sayouti, "Optimal sizing and cost of a microgrid based in PV, Wind and BESS for a school of engineering," in *Proceedings of International Conference on Wireless Technologies*, *Embedded and Intelligent Systems*, Fez, Morocco, Apr. 2017, pp. 1-5.
[34] M. Nazari-Heris, B. Mohammadi-Ivatloo, S. Asadi *et al*., "Large-scale combined heat and power economic dispatch using a novel multi-player harmony search method," *Applied Thermal Engineering*, vol. 154, pp. 493-504, May 2019.
[35] O. Hoseynpour, B. Mohammadi-Ivatloo, M. Nazari-Heris *et al*., "Application of dynamic non-linear programming technique to nonconvex short-term hydrothermal scheduling problem," *Energies*, vol. 10, no. 9, p. 1440, Sept. 2017.
[36] R. Kumar, R. Gupta, and A. K. Bansal, "Economic analysis and power management of a stand-alone wind/photovoltaic hybrid energy system using biogeography based optimization algorithm," *Swarm and Evolutionary Computation*, vol. 8, pp. 33-43, Feb. 2013.
[37] M. Nazari-Heris, A. F. Babaei, B. Mohammadi-Ivatloo *et al*., "Improved harmony search algorithm for the solution of non-linear non-convex short-term hydrothermal scheduling," *Energy*, vol. 151, pp. 226-237, May 2018.
[38] O. Ekren and B. Y. Ekren, "Size optimization of a PV/wind hybrid energy conversion system with battery storage using simulated annealing," *Applied Energy*, vol. 87, no. 2, pp. 592-598, Feb. 2010.
[39] D. Karaboga and B. Akay, "A comparative study of artificial bee colony algorithm," *Applied Mathematics and Computation*, vol. 214, no. 1, pp. 108-132, Aug. 2009.
[40] D. Karaboga and B. Basturk, "A powerful and efficient algorithm for numerical function optimization: artificial bee colony algorithm," *Journal of Global Optimization*, vol. 39, no. 3, pp. 459-471, Nov. 2007.
[41] J. Kennedy and R. Eberhart, "Particle swarm optimization," in *Proceedings of ICNN'95-International Conference on Neural Networks*, Perth, Australia, Mar. 1995, pp. 1942-1948.
[42] Surface meteorology and solar energy. (2019, Dec.). [Online]. http://eosweb.larc.nasa.gov/sse/RETScreen, NASA
[43] HOMER. (2019, Dec.). [Online]. https://www.homerenergy.com/products
[44] S. Singh and S. C. Kaushik, "Optimal sizing of grid integrated hybrid PV-biomass energy system using artificial bee colony algorithm," *IET Renewable Power Generation*, vol. 10, no. 5, pp. 642-650, Apr. 2016.
[45] N. J. Singh, J. S. Dhillon, and D. P. Kothari, "Synergic predatorprey optimization for economic thermal power dispatch problem," *Applied Soft Computing*, vol. 43, pp. 298-311, Jun. 2016.

Shakti Singh received the B.E. and M.Tech. degrees in electrical engineering and energy from Madan Mohan Malviyan Engineering College, Gorakhpur and Indian Institute of Technology, Delhi, India, respectively. He holds a Ph.D. degree in optimization of hybrid renewable energy systems. He is currently working as an Assistant Professor with Electrical and Instrumentation Engineering Department, Thapar Institute of Engineering and Technology, Patiala, India. His research interests include grid integration of renewable energy sources, distributed power generation, and microgrid.

Prachi Chauhan received her B.Tech. degree in electrical and electronics engineering and M.Tech. degree in power systems, from College of Engineering Roorkee, Roorkee, India, and Thapar Institute of Engineering and Technology, Patiala, India, in 2017 and 2019, respectively. Her research interests include modeling of hybrid renewable energy system and electric vehicles.

Nirbhow Jap Singh received the B.E. and M.E. degrees in instrumentation and control engineering from Sant Longowal Institute of Engineering and Technology, Sangrur, Punjab, India. He received his Ph.D. degree in system optimization algorithms from Thapar Institute of Engineering and Technology Patiala, Punjab, India. He is currently working as an Assistant Professor in Electrical and Instrumentation Engineering Department, Thapar Institute of Engineering and Technology, Patiala, India. His research interests include embedded system design, artificial intelligence applications, and engineering optimization algorithms.